A global stability analysis of a thin-airfoil wake

Jan Oscar Pralits, Flavio Giannetti, Paolo Luchini
Department of Mechanical Engineering, University of Salerno, Italy
E-mail: jpralits@unisa.it, fgiannetti@unisa.it, luchini@unisa.it

Keywords: Fluid mechanics, thin airfoil, stability analysis, global modes, structural sensitivity.

SUMMARY. In this paper we review the problem of the wake-flow stability for a thin airfoil by using both a locally plane-wave analysis, based on a WKBJ approximation, and a global numerical stability analysis. The core of the instability is further localized by performing a structural sensitivity analysis of the linearized Navier-Stokes operator as outlined in [7]. In particular the sensitivity of the eigenvalue to a spatially-localized feedback from velocity to force is evaluated by using the product of the direct and adjoint global mode. It is shown, using a plane wave analysis, that the flow at the trailing edge is absolutely unstable for any Reynolds number for values of the parameter m corresponding to separation of the base flow. The analysis further shows that the base flow at the trailing edge is not absolutely unstable as the value of m tends to zero. The global eigenvalue analysis shows that the frequency and growth rate are very similar to what is found with the local plane wave analysis at the trailing edge. Finally, the structural sensitivity analysis indicates that the wavemaker is situated just downstream of the trailing edge. .

1 INTRODUCTION

The problem of wake-flow instability behind a flat plate or thin airfoils has been the subject of many analytical and numerical studies. The first investigations of the stability of these flows dealt with the flat plate geometry and the characteristics of the wake behind the trailing edge were modeled with analytical profiles. An example is offered by the work of [1] who solved the temporal and spatial linear instability problems, both numerically for order-one growth rates and analytically for the small- and large-wavenumbers. Their results are in good agreement with the experimental results of [2]. In this and other experiments the focus was on convective-type instabilities which were forced by loudspeaker excitation of the flow. Self-excited oscillations in the wake of a thin airfoil were successively examined by [3] and [4] who used the theory of absolute instability, as discussed by [5], to investigate the global stability characteristics of the flow. By numerically integrating the boundary layer equations on a thin airfoil they showed that the flow at the trailing edge can be well modeled by a double Falkner-Skan profile with an adverse pressure gradient. Their analysis shows that in a given range of parameters the wake becomes globally unstable, promoting the development of a Karman vortex shedding. The frequency of the global oscillation was determined, in [3], at leading order using a multiple-scales-type WKBJ analysis, assuming the flow to be slowly varying in the streamwise direction. More recently [6] repeated the analysis on the thin airfoil wake in order to investigate the nonlinear development of the perturbation and locate the front of the nonlinear global mode.

In this paper we review the problem of the wake-flow stability for a thin airfoil by using both a locally plane-wave analysis, based on a WKBJ approximation, and a global numerical stability analysis and compare our results with those by [3]. The core of the instability is further localized by performing a structural sensitivity analysis of the linearized Navier-Stokes operator as outlined in [7]. In particular the sensitivity of the eigenvalue to a spatially-localized feedback from velocity to force is evaluated by using the product of the direct and adjoint global mode. In such way, the

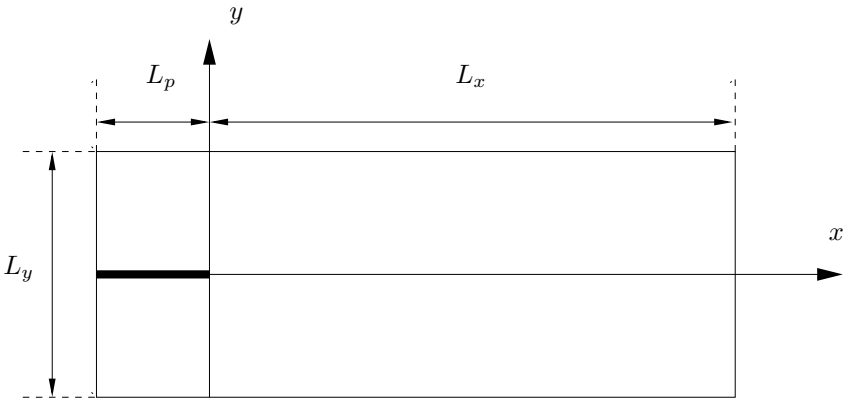

Figure 1: Computational domain where L_p is the length of the final part of the airfoil before the trailing edge.

position of the "wavemaker" of the asymptotic theory can be determined by inspecting where in space the sensitivity reaches its maximum level.

2 PROBLEM FORMULATION

The aim of this study is to investigate the stability characteristics of the wake-flow behind an airfoil. It is assumed that the airfoil is thin and symmetric such that the flow at the trailing edge can be well approximated by the Falkner-Skan similarity solution, as discussed by [3]. In both [3] and [4], performing a local stability analysis, it was found that for certain values of the Reynolds number and pressure gradient the flow is absolutely unstable at the trailing edge. In order to avoid an absolutely unstable flow at the inlet of the computational domain we have added a flat plate of infinitesimal thickness upstream of the trailing edge in order to model the downstream part of the airfoil. The computational domain is given in figure 1 showing the Cartesian coordinate system with its origin at the trailing edge. The domain is characterized by three different lengths: the downstream part of the airfoil denoted L_p, the length of the computational domain downstream of the trailing edge L_x and the domain height L_y.

2.1 Governing equations

The wake flow is described by the two-dimensional unsteady incompressible Navier-Stokes equations

$$\frac{\partial \mathbf{U}}{\partial t} + \mathbf{U} \cdot \nabla \mathbf{U} = -\nabla P + \frac{1}{Re} \Delta \mathbf{U}, \tag{1}$$

$$\nabla \cdot \mathbf{U} = 0, \tag{2}$$

where $\mathbf{U}$ is the velocity vector with components $\mathbf{U} = (U, V)$ and P is the reduced pressure. Equations (1)–(2) are given the following boundary conditions. Two Falkner Skan similiarity solutions are used as an inlet condition at $x = -L_p$ and the non-slip condition is used on both sides of the flat plate. In the far field the flow approaches the incoming uniform stream, that is $\mathbf{U} \rightarrow (U_\infty, 0)$ as $y \rightarrow \pm\infty$. The Falkner-Skan solution is a function of the pressure gradient which is expressed by the power-law parameter m. The characteristic length scale is taken to be the displacement thickness

$\delta^\star$ of the inlet profile. The two parameters which define the present configuration are the Reynolds number $Re = \frac{U^\star_\infty \delta^\star}{\nu^\star}$ and power-law parameter m.

3 LOCAL STABILITY ANALYSIS

The analysis in this section is made considering steady parallel flow in the x direction. In the first part we analyse the stability characteristics of the base flow at the trailing edge ($x = 0$) where the steady flow is taken as the Falkner Skan similarity solution. In a next step we perform a local stability analysis of the steady base flow obtained as the solution of the steady version of equation (1)-(2).

The stability problem for a strictly parallel, viscous two-dimensional flow is described by the Orr-Sommerfeld equation, which is written in terms of the unsteady velocity perturbation $v(x, y, t) = \hat{v}(y) \exp(-i\omega t + i\alpha x)$ in the form

$$\left[(i\alpha U_b - i\omega) \left(\frac{\partial^2}{\partial y^2} - \alpha^2 \right) - i\alpha U_b'' \right] \hat{v} = \frac{1}{Re} \left(\frac{\partial^2}{\partial y^2} - \alpha^2 \right)^2 \hat{v}, \tag{3}$$

where ω and α are the angular frequency and streamwise wave number, respectively, U_b is the steady base flow and the superscript prime denotes the derivative in the y direction. In the free stream we impose asymptotic boundary conditions derived from (3) by considering a constant base flow. At $y = 0$ the base flow is discontinuous in the derivatives. It is therefore necessary to impose boundary conditions for the perturbations which take into account of this discontinuity. Two possible solutions are found; symmetric and antisymmetric modes. The boundary conditions for these two solutions are given as

$$\hat{v}(0) = \hat{v}''(0) = 0, \tag{4}$$

$$\hat{v}'(0) = \hat{v}'''(0) + i\alpha Re U_b'(0)\hat{v}(0) = 0, \tag{5}$$

respectively.

3.1 Absolute instability

It has already been found in previous investigations, for example [3] and [4], that no absolute instability is obtained for the symmetric modes. This has been confirmed with our own computations and we therefore only investigate the antisymmetric case (5) here. The absolute instability, as defined by [8] in plasma physics when studying the causal response to impulsive forcing, arises when two (or more) spatial modes originating in opposite half planes pinch together as the temporal contour is lowered towards the real axis. This pinch corresponds to an unstable mode with zero group velocity, and hence to disturbances which grow in time at a fixed point in space and potentially lead to nonlinear behavior. We can define the absolute instability ω_0 as

$$\omega_0 = \omega(\alpha_0) \qquad \text{with} \qquad \frac{\partial \omega}{\partial \alpha}(\alpha_0) = 0. \tag{6}$$

3.2 Numerical results

Equation (3) together with boundary conditions (5) are discretized using second order finite differences on a uniform grid. The eigenvalue ω for a given α and Reynolds number is computed using an inverse iteration procedure. The absolute instability is calculated using a Newton procedure in order to find the streamwise wavenumber α which satisfies (6).

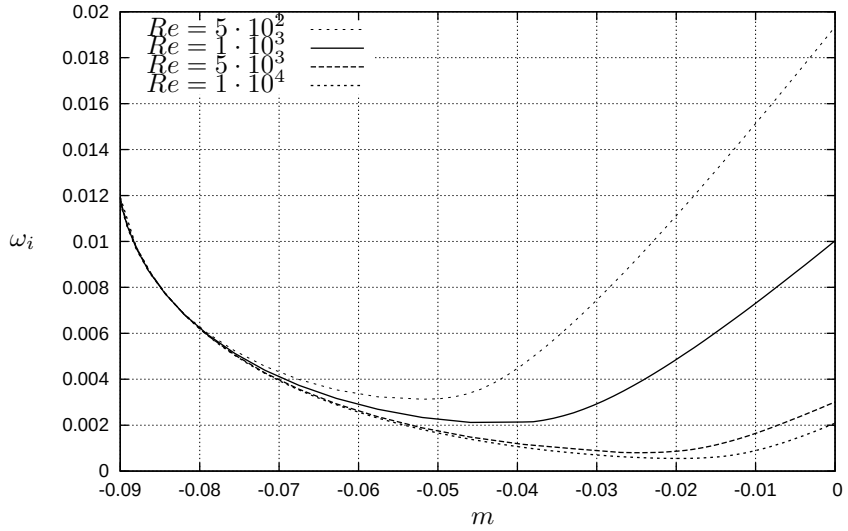

Figure 2: Growth rate of instability of type 1 at saddles as a function of the the parameter m for different Reynolds numbers computed at $x = 0$.

The results shown here have been obtained using the same values for the Reynolds number and power-law parameter m as in [4] for comparison. In figure 2 the growth rate of the least stable mode is shown for different Reynolds numbers and values of m between zero and -0.09. Note that -0.09 is close to value which corresponds to separation of the base flow. In all cases the condition (6) is satisfied and the growth rate is positive. For values of m close to separation the value of the growth rate is independent of the Reynolds number. Further, for large Reynolds numbers the growth rate tends to zero as value of m approaches that of the Blasius boundary layer ($m = 0$). However, for lower Reynolds numbers is seems to exist a value for m above which the growth rate increases implying that the Blasius boundary layer is absolutely unstable.

This is however not true, as also shown by [4], since another saddle point exists at which the mode satisfying condition (6) is unstable and both solutions must be considered in order to have the correct causal response to impulsive forcing. We denote, as in [4], the solution shown in figure 2 type I saddles. The second solution, denoted type II saddles, is shown in figure 3 for different values of m and *Re*. It is found that this solution is stable for base flows close to separation and for values of m close to zero. Moreover, for certain values of m and *Re* both solutions are unstable.

In order to better understand these different saddle points we analyse in detail two different points in the m-*Re* plane. The values are $(\mathit{Re}, m) = (1000, -0.02)$ and $(\mathit{Re}, m) = (1000, -0.06)$. The Reynolds number has been chosen small enough such that the growth rate for $m = -0.02$ is clearly larger with respect to the large Reynolds number limit for the type I saddle. For both cases the growth rate has been computed for different values of the complex streamwise wave number α. The results are shown in figures 4 and 5 where dashed and solid contours show negative and positive growth rate respectively. It can be seen that the two saddle points with positive growth rate shown in figures 2 and 3 have been captured for each case.

It turns out that the type I saddles change from pinching to non-pinching above a certain value of m for each *Re* and therefore do not lead to an absolute instability, and this is due to their interaction

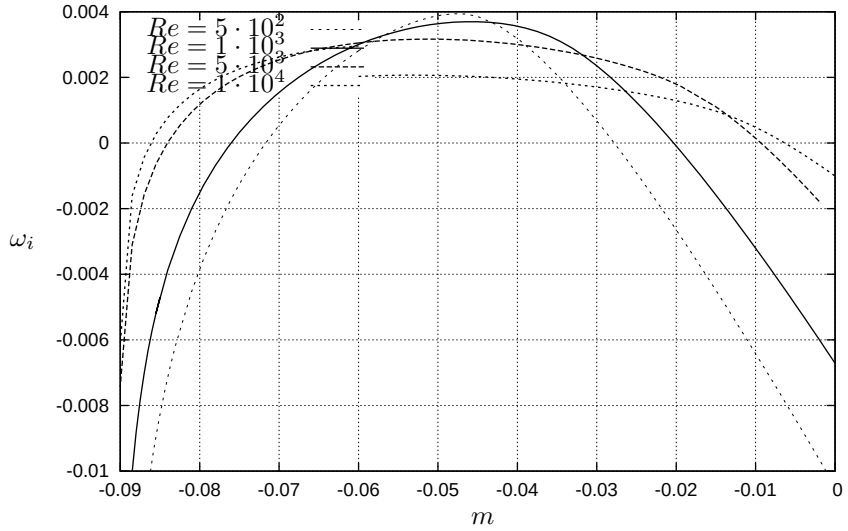

Figure 3: Growth rate of instability of type 2 at saddles as a function of the the parameter m for different Reynolds numbers computed at $x = 0$.

with type II saddles which are always pinching. Note that "pinch" defines modes coalescing from opposite spatial half planes while non-pinching means that the two modes coalesce from the upper half plane. In both cases the long time behavior is determined by the pinching saddle with the largest growth rate. For the $m = -0.06$ case both saddles are pinching and the type I mode has the largest growth rate. In the $m = -0.02$ case only the type II mode is pinching and therefore determines the long time behavior. This analysis has been made for different m and *Re* it can be concluded that non absolute instability exists as m tends to zero.

The streamwise evolution of the absolute instability in the airfoil wake has also been computed. This was made by first solving the steady version of equations (1)-(2) in order to obtain the steady base flow. The absolute instability was then computed for at each streamwise position in order to obtain its streamwise evolution. An example is given in figure 6 for *Re* $= 2000$, $m = -0.09$ and $L_x = 120$. It can be seen that the maximum growth rate is found at the trailing edge and that the mode becomes stable at $x \approx 95$.

3.3 Global instability

The complex global frequency ω_g is obtained by the saddle-point condition

$$\omega_g = \omega_0(x_s) \quad \text{where} \quad \frac{\partial \omega_0}{\partial x}(x_s) = 0$$

based on the analytic continuation of the local absolute frequency curve $\omega_0(x)$ in the complex x-plane, with x_s denoting the slow streamwise variable at the saddle point.

4 GLOBAL STABILITY ANALYSIS

In order to validate the results based on the asymptotic theory, a fully numerical global stability analysis of the thin-airfoil wake is performed. The instability onset is studied using linear theory and

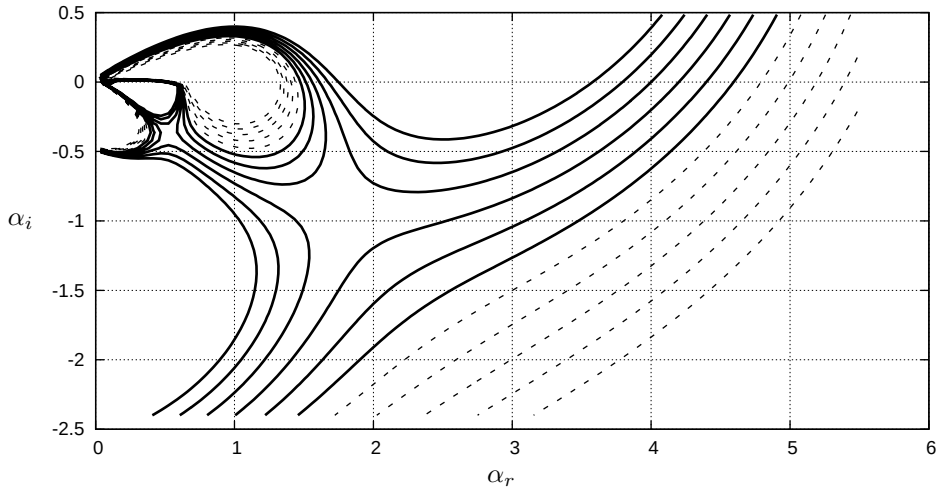

Figure 4: Contours of growth rate ω_i: negative (dashed) and positive (solid), for $Re = 1000$ and $m = -0.06$.

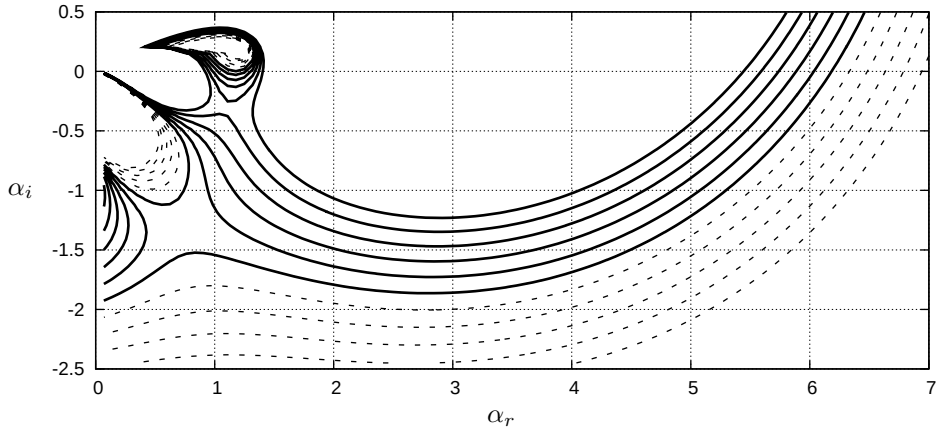

Figure 5: Contours of growth rate ω_i: negative (dashed) and positive (solid), for $Re = 1000$ and $m = -0.02$.

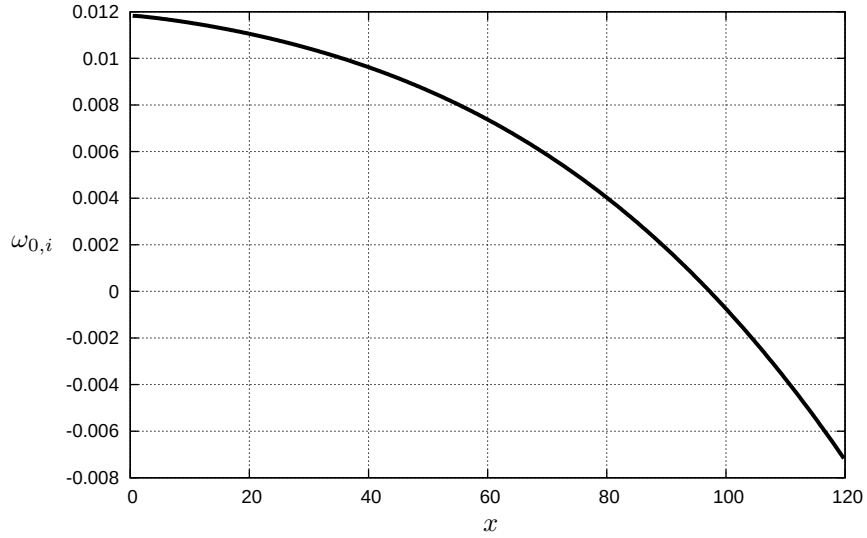

Figure 6: Growth rate the of absolute instability ω_0 as a function of the streamwise coordinate x for the case when $Re = 2000$ and $m = -0.09$.

a normal-mode analysis. The flow quantities are decomposed in a steady part and a small unsteady perturbation as $\mathbf{U}(x, y, t) = \mathbf{U}_b(x, y) + \epsilon\mathbf{u}(x, y, t)$ and $P(x, y, t) = P_b(x, y) + \epsilon p(x, y, t)$, where the amplitude ϵ is assumed to be small. Since we are interested in two-dimensional global modes an ansatz is used such that $\mathbf{u}(x, y, t) = \hat{\mathbf{u}}(x, y)\exp(\sigma t)$ and $p(x, y, t) = \hat{p}(x, y)\exp(\sigma t)$. Introducing the flow decomposition and the ansatz into equations (1)-(2) and linearising we obtain the linearised unsteady Navier-Stokes equations

$$\sigma\hat{\mathbf{u}} + \mathbf{L}\{\mathbf{U}_b, Re\}\hat{\mathbf{u}} + \boldsymbol{\nabla}\hat{p} = \mathbf{0}, \tag{7}$$

$$\boldsymbol{\nabla}\cdot\hat{\mathbf{u}} = 0, \tag{8}$$

where the base flow is the solution of the steady version of (1)–(2) and

$$\mathbf{L}\{\mathbf{U}_b, Re\}\hat{\mathbf{u}} = \mathbf{U}_b\cdot\boldsymbol{\nabla}\hat{\mathbf{u}} + \hat{\mathbf{u}}\cdot\boldsymbol{\nabla}\mathbf{U}_b - \frac{1}{Re}\Delta\hat{\mathbf{u}}. \tag{9}$$

On both sides of the plate, $-L_p < x < 0$ and $y = 0$, a no-slip boundary condition is imposed while in the far field appropriate radiative boundary conditions are used, see [7]. At the outflow a zero normal stress condition is imposed. At the upstream boundary, the vorticity is set to zero while the streamwise velocity component is required to vanish. Similarly, on the upper and lower boundary, the normal velocity component v is assumed to decay and the vorticity is set to zero. The system (7)–(8) gives rise to a generalised eigenvalue problem for the complex eigenvalue σ. For $\mathrm{Re}(\sigma) < 0$ the flow is stable while for $\mathrm{Re}(\sigma) > 0$ the mode is unstable and grows exponentially in time.

4.1 Numerical method

The results presented here are obtained with the numerical code described in [7]. A second-order finite-difference approach is used to compute spatial derivatives of the governing partial differential equations together with an immersed-boundary technique to represent the cylinder surface on

a Cartesian mesh. The computational domain is rectangular. With the spatial discretisation and boundary conditions described above two different problems are addressed. First, the steady non-linear Navier-Stokes equations (1)–(2) are solved by Newton iteration in order to compute the base flow used for the linear stability analysis. Second, the stability of the flow is investigated through the eigenvalue problem defined by the linearised perturbation equations (7)–(8), where an inverse iteration algorithm is implemented to compute the least stable eigenvalue and eigenmode, see [7] for further details on the numerical approach.

5 SENSITIVITY ANALYSIS

The sensitivity of the unstable shedding mode is used to identify the core of the instability. In weakly non-parallel flows the WKBJ approach enables to identify a specific spatial position in the absolutely unstable region which acts as a wave-maker, determining e.g. the oscillation frequency by the saddle point criterion [10, 11, 9]. For more complex configurations strong non-parallel effects prevent us from using the asymptotic theory and a global analysis is necessary. In this context, a concept similar to that of wave-maker can be introduced by investigating where in space a modification in the structure of the problem produces the largest drift of the eigenvalue: this is done by determining the region where feedback from velocity to force is most effective. The derivation is briefly outlined here for continuous operators and further details can be found in [7].

We consider the perturbed eigenvalue problem satisfying the equations

$$\sigma' \hat{\mathbf{u}}' + \mathbf{L}\{\mathbf{U}_b, Re\}\hat{\mathbf{u}}' + \boldsymbol{\nabla}\hat{p}' = \delta\mathbf{M}(x,y)\cdot\mathbf{u}', \tag{10}$$

$$\boldsymbol{\nabla}\cdot\hat{\mathbf{u}}' = 0, \tag{11}$$

where the right hand side of (10) is a structural perturbation localised in space in the form of a local force proportional to a local velocity and

$$\delta\mathbf{M}(x,y) = \delta(x-x_0, y-y_0)\,\delta\mathbf{M}_0,$$

where $\delta\mathbf{M}_0$ is a 2 by 2 matrix of the coupling coefficients expressing the particular form of the localised structural perturbation and $\delta(x-x_0, y-y_0)$ stands for the Kronecker delta function. The eigenvalue drift $\delta\sigma$ and corresponding variation of the eigenfunctions with respect to the unperturbed problem can be derived using the expansion $\hat{\mathbf{u}}' = \hat{\mathbf{u}} + \delta\hat{\mathbf{u}}$ and $\hat{p}' = \hat{p} + \delta\hat{p}$. Introducing the perturbation decomposition into (10)-(11) and further the Lagrange identity, as in [7], we can express the eigenvalue drift due to the local feedback as

$$\delta\sigma(x_0,y_0) = \frac{\displaystyle\int_\Omega \hat{\mathbf{f}^+}\cdot\delta\mathbf{M}\cdot\hat{\mathbf{u}}\,dS}{\displaystyle\int_\Omega \hat{\mathbf{f}^+}\cdot\hat{\mathbf{u}}\,dS} = \frac{\hat{\mathbf{f}^+}\cdot\delta\mathbf{M}_0\cdot\hat{\mathbf{u}}}{\displaystyle\int_\Omega \hat{\mathbf{f}^+}\cdot\hat{\mathbf{u}}\,dS} = \mathbf{S}:\delta\mathbf{M}_0 = \sum_{ij} S_{ij}\,\delta M_{0ij}, \tag{12}$$

where

$$\mathbf{S}(x_0,y_0) = \frac{\hat{\mathbf{f}^+}(x_0,y_0)\,\hat{\mathbf{u}}(x_0,y_0)}{\displaystyle\int_\Omega \hat{\mathbf{f}^+}\cdot\hat{\mathbf{u}}\,dS}. \tag{13}$$

Here $\mathbf{g}^+ \equiv \{\mathbf{f}^+, m^+\}$ satisfy the adjoint equations given in [7]. In the above expression the notation $\hat{\mathbf{f}^+}\,\hat{\mathbf{u}}$ indicates the dyadic product between the direct and adjoint modes. Different norms of the tensor $\mathbf{S}$ can be used to build a spatial map of the sensitivity. The spectral norm is chosen here to study the worst possible case.

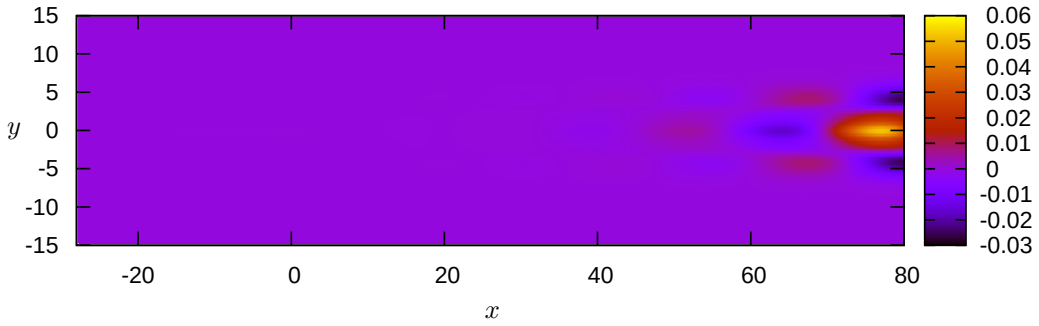

Figure 7: Real part of the vorticity of the least stable global mode for $Re = 2000$ and $m = -0.09$.

5.1 Numerical results

The results presented here have been computed for *Re* $= 2000$ and $m = -0.09$. The dimensions of the domain used are $L_p = 28$, $L_x = 120$ and $L_y = 50$. In figure 7 the real part of the vorticity is shown and the usual Karman vortex pattern can be observed in the downstream part of the domain. The global frequency and growth rate are 0.163 and 0.0193, respectively, which are quite similar to the values of the absolute instability at the trailing edge for the same parameters, namely 0.161 and 0.012. In figure 8 the structural sensitivity is plotted. It can clearly be seen that the maximum is localised in the vicinity, just downstream, of the trailing edge.

6 Conclusions

In this paper we have reviewed the problem of the wake-flow stability for a thin airfoil by using both a locally plane-wave analysis, based on a WKBJ approximation, and a global numerical stability analysis. The core of the instability has further been localized by performing a structural sensitivity analysis of the linearized Navier-Stokes operator as outlined in [7]. In particular the sensitivity of the eigenvalue to a spatially-localized feedback from velocity to force is evaluated by using the product of the direct and adjoint global mode. In such way, the position of the "wavemaker" of the asymptotic theory can be determined by inspecting where in space the sensitivity reaches its maximum level.

It has been shown, using a plane wave analysis, that the flow at the trailing edge is absolutely unstable for any Reynolds number for values of the parameter m corresponding to separation of the base flow. The analysis further shows that the base flow at the trailing edge is not absolutely unstable as the value of m tends to zero.

The global eigenvalue analysis shows that the frequency and growth rate are very similar to what is found with the local plane wave analysis at the trailing edge. Finally, the structural sensitivity analysis indicates that the wavemaker is situated just downstream of the trailing edge.

References

[1] Papageorgiou, D. T. ,Smith, F.T., “Linear stability of the wake behind a flat plate placed parallel to a uniform stream,” *J. Fluid Mech.*, **208**, 67-89 (1989).

[2] Mattingly, G.E. , Criminale, W.O., “The stability of an incompressible two-dimensional wake,” *J. Fluid Mech.*, **51**, 233-272 (1972).

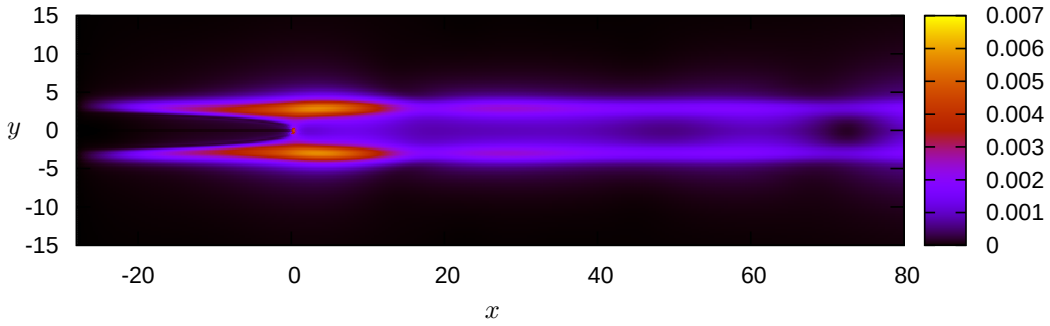

Figure 8: Real part of the vorticity of the least stable global mode for $Re = 2000$ and $m = -0.09$.

[3] Woodley, B.M. , Peake, N., "Global linear stability analysis of thin airfoil wakes," *J. Fluid Mech.*, **339**, 239-260 (1997).

[4] Taylor, M.J., Peake, N., "A note on the absolute instability of wakes," *Eur. J. Mech. B/Fluids*, **18**, 573-579 (1999).

[5] Huerre, P. , Monkewitz, P. A. , "Local and global instabilities in spatially developing flows," *Ann. Rev. Fluid Mech.*, **22**, 473-537 (1990).

[6] Peake, N., Pier, B., "Global nonlinear dynamics of thin aerofoil wakes," in *Book of abstract of the European Fluid Mechanics Conference*, Manchester, U.K., September 14-18, (2008).

[7] Giannetti, F., Luchini, P., "Structural Sensitivity of the first instability of the cylinder wake," *J. Fluid Mech.*, **581**, 167-197 (2007).

[8] Briggs, R., "Electron-Stream Interaction with Plasmas," *MIT Press*, (1964).

[9] Chomaz, J.-M., "Global instabilities in spatially developing flows: Non-normality and nonlinearity," *Annu. Rev. Fluid Mech.* **37**, 357-392 (2005).

[10] Chomaz, J. M., Huerre, P. & Redekopp, L. G., "A frequency selection criterion in spatially developing flows," *Stud. Appl. Math.* **84**, 119-144 (1991).

[11] Dizés, S. L., Huerre, P., Chomaz, J. & Monkewitz, P., "Linear global modes in spatially developing media," *Phil. Trans. R. Soc. Lond. A* **354** (1705), 169–212 (1996).